

DIBOSONS AT THE TEVATRON

THOMAS J. PHILLIPS

*Department of Physics, Duke University,
Durham, NC 27708-0305 USA*



Diboson events produced by $p\bar{p}$ collisions at $\sqrt{s} = 1.96$ TeV at the Fermilab Tevatron have been studied by the CDF and D0 collaborations. The mechanism of electroweak symmetry breaking in the Standard Model results in triple gauge couplings between W bosons and both photons and Z bosons, but predicts no tree-level couplings between photons and the Z boson or Z -boson self-couplings. Observations of $W\gamma$, $Z\gamma$, WW , WZ , and ZZ production are consistent with Standard Model predictions, and limits are set on some anomalous couplings. In addition, searches for resonant production of dibosons have been used to set limits on new physics.

1 Introduction

The electroweak symmetry breaking mechanism of the Standard Model produces a limited set of couplings that involve three vector bosons. Specifically, there are vertices that include two W bosons and either a photon or a Z boson, but there are no vertices that just contain combinations of photons and Z bosons. However, extension of the Standard Model can contain these “anomalous” couplings as well as anomalous couplings between Z -bosons or photons and W bosons.

The study of events with two vector bosons (“diboson” events) provides a sensitive probe of these couplings and therefore provides a sensitive test of fundamental Standard Model physics. There are t -channel diagrams for diboson production ($W\gamma$, $Z\gamma$, WW , WZ , and ZZ), but only $W\gamma$, WW , and WZ have s -channel diagrams. This paper describes studies of the production characteristics of diboson events at the Tevatron by the CDF and D0 collaborations which have compared measured cross sections to Standard Model predictions and have set limits on anomalous couplings.

Table 1: Cross sections (in picobarns) for dibosons at the Tevatron.

Diboson	Expt.	Measured	SM Prediction
$W\gamma, E_{T\gamma} > 7 \text{ GeV}$	CDF	18.0 ± 2.8	19.3 ± 1.4
$W\gamma, E_{T\gamma} > 8 \text{ GeV}$	D0	14.8 ± 2.1	16.0 ± 0.4
$Z\gamma, E_{T\gamma} > 7 \text{ GeV}$	CDF	4.6 ± 0.5	4.5 ± 0.4
$Z\gamma, E_{T\gamma} > 90 \text{ GeV}$	D0	$0.032 \pm 0.009 \pm 0.002$	0.039 ± 0.004
WZ	CDF	$4.3 \pm 1.4 \pm 1.1$	3.65 ± 0.25
WZ	D0	$2.7^{+1.7}_{-1.3}$	3.68 ± 0.25
WW	CDF	$13.6 \pm 2.3 \pm 1.6 \pm 1.2$	12.4 ± 0.8
WW	D0	$11.8^{+3.7+1.0}_{-3.2-0.8} \pm 0.7$	12.0 to 13.5
ZZ	CDF	$1.4^{+0.7}_{-0.6}$	1.4 ± 0.1
ZZ	D0	1.6 ± 0.7	1.4 ± 0.1

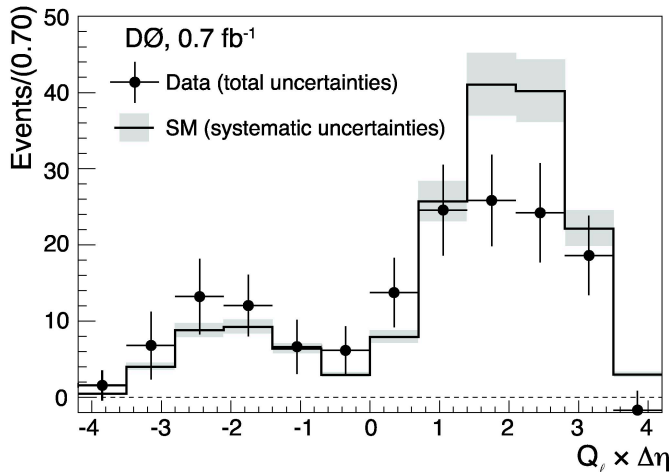


Figure 1: Rapidity difference (times charge) between lepton and photon in $W\gamma$ events at D0. The dip in the center is due to a radiation-amplitude zero created by the interference of production diagrams.

2 Diboson Production at the Tevatron

2.1 $W\gamma$ Production

Because of infrared divergences, the cross sections for $W\gamma$ and $Z\gamma$ production depend upon the energy threshold applied to the photon and upon the separation required between the photon and the charged leptons from the boson decays. CDF used a threshold of $E_T^\gamma > 7 \text{ GeV}$ while D0 used a threshold of $E_T^\gamma > 8 \text{ GeV}$. The measured cross sections are shown in Table 1 and they are consistent with Standard Model predictions.

A particularly interesting aspect of Standard Model $W\gamma$ production is that the interference between production diagrams gives a particular angle at which no radiation is produced, a radiation-amplitude zero (RAZ). This RAZ was first predicted thirty years ago¹ and D0 recently claimed observation². The predicted and measured distributions of the lepton-photon rapidity difference are shown in Fig. 1.

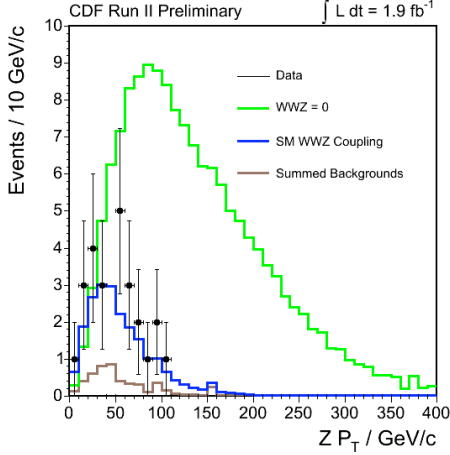


Figure 2: P_T distribution of Z bosons in WZ events. The green curve shows the expected distribution if there were no WWZ vertex. The blue curve is the SM expectation including interference from this vertex. The points are the CDF data.

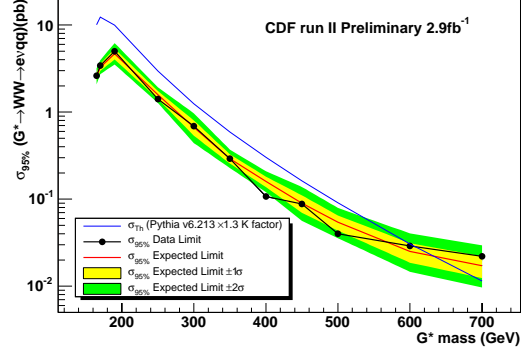


Figure 3: Cross section limit on R/S gravitons.

2.2 WW and WZ Production

Interference also plays a role in the Standard Model prediction for WZ production. If there were no WWZ vertex, the t -channel by itself would produce many more events and with a harder Z P_T distribution than is predicted when s -channel production is included. These predictions are shown in Fig. 2 along with the CDF observation, which is consistent with the SM prediction and clearly inconsistent with the prediction without the WWZ coupling.

Both D0 and CDF have measured the cross section for WW and WZ production as shown in Table 1 and again the measurements are consistent with SM predictions. In addition, both experiments have set limits on anomalous couplings, couplings that differ in form from the SM predictions. These couplings are usually parameterized as $\Delta\kappa$, Δg , and λ ³. For WZ production, D0 evaluates these at a scale $\Lambda = 2$ TeV and finds⁴ $-0.12 < \Delta\kappa_Z (= \Delta g_1^Z) < 0.29$ and $-0.17 < \lambda_Z < 0.21$, while CDF does not constrain $\Delta\kappa = \Delta g$ and finds $-0.13 < \lambda < 0.14$, $-0.76 < \Delta\kappa < 1.18$, and $-0.13 < \Delta g < 0.23$. Similarly, for WW production, at a scale of $\Lambda = 2$ TeV and under the assumption that $WW\gamma$ couplings are equal to WWZ couplings, D0 finds⁵ the limits $-0.32 < \Delta\kappa < 0.45$ and $-0.29 < \lambda < 0.30$.

The above cross sections and anomalous coupling limits were measured for events where both W 's and Z 's decayed leptonically. Both experiments have also looked for events where one W decayed leptonically on the other W or Z decayed to dijets^{6,7}. This is of particular interest if there is resonance production of a particle that decays into WW or WZ , which would be a clear indication of new physics. CDF has a preliminary result, shown in Fig. 3, where a search for a WW resonance was used to set a 95% C.L. lower limit on the mass of an R/S graviton, G^* , ($k/\text{mp}=0.1$) of 607 GeV/ c^2 . Limits were also set excluding a Z' between 247 and 545 GeV/ c^2 and a W' between 284 and 515 GeV/ c^2 at the 95% C.L.

2.3 $Z\gamma$ Production

As is the case for $W\gamma$, the $Z\gamma$ cross section depends upon the E_T^γ threshold chosen. CDF measured the cross section for $E_T^\gamma > 7$ GeV, as with $W\gamma$, and D0's most recent measurement⁸ is for $E_T^\gamma > 90$ GeV. This high threshold is used so that Z -bosons that decay to neutrino pairs could be detected using missing transverse energy. The branching ratio for the Z to decay to

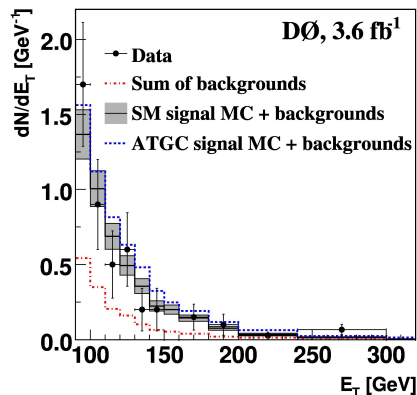


Figure 4: E_T distribution for single unbalanced, isolated photons. These are dominated by $Z\gamma$ events where the Z has decayed to neutrino pairs.

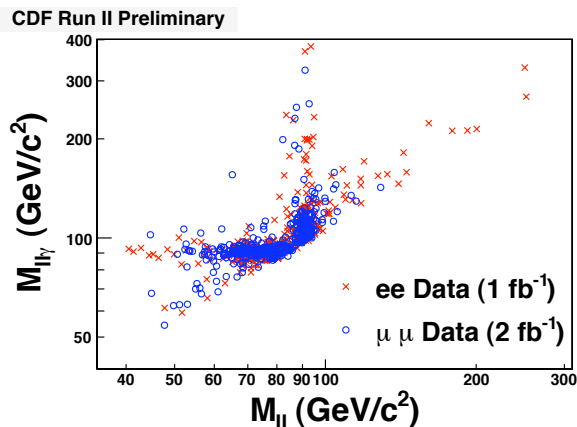


Figure 5: Two-body vs. three-body mass for $Z\gamma$ events. Initial-state-radiation events cluster around $M_{ll} = 91\text{GeV}/c^2$ while final-state-radiation events cluster around $M_{ll\gamma} = 91\text{GeV}/c^2$.

neutrinos is about six times higher than the branching ratio into either electron or muon pairs, so even though there is substantial background, the additional statistics for high E_T^γ are important, especially when calculating anomalous coupling limits since the anomalous couplings produce more events at high E_T^γ . The E_T^γ distribution for the events found by D0 is shown in Fig. 4. The measured cross sections are shown in Table 1 and they are again consistent with Standard Model predictions.

The Standard Model does not contain a coupling between the Z boson and a photon, nor does it contain a vertex with three Z bosons. Both CDF and D0 have produced limits on these anomalous couplings. Because of unitarity, these anomalous coupling limits depend upon scale factors. The CDF limits are based upon $1\text{-}2\text{ fb}^{-1}$ of data and were calculated using a scale of $\Lambda = 1.2\text{ TeV}$, and they are $|h_{30}^Z| < 0.083$, $|h_{30}^\gamma| < 0.084$, and $|h_{40}^{\gamma,Z}| < 0.047$. The D0 results use a similar amount of data and also include 3.6 fb^{-1} of $Z \rightarrow \nu\nu$ data. D0 uses a scale factor of $\Lambda = 1.5\text{ TeV}$, and the limits are $|h_{30}^{\gamma,Z}| < 0.033$ and $|h_{40}^{\gamma,Z}| < 0.0017$.

For $Z\gamma$ events where the Z decays to electrons or muons it is instructive to plot the three-body mass $ll\gamma$ against the two body mass ll , as shown in Fig. 5. There are two clusters of events: those where the three-body $ll\gamma$ mass is approximately the Z mass, which are predominantly from final-state radiation where the photon is radiated off one of the leptons, and those where the two-body ll mass is approximately the Z mass, which is dominated by initial-state radiation where the photon is radiated off one of the incoming quarks. We note that events produced by anomalous couplings will populate the initial-state radiation region, since the $Z \rightarrow ll$ will be on the mass shell.

2.4 ZZ Production

The last of the diboson varieties to be seen at the Tevatron was ZZ . Not only is the production cross section expected to be small (only 1.4 pb), but the Z also has a small branching fraction into charged leptons, so the probability for both Z 's to decay into charged leptons, the only Z decays that can be unambiguously identified, is the square of this small branching fraction. The experiments have found three events each consistent with ZZ decaying into four charged leptons; CDF has found two events with four muons and one with four electrons, while D0 has found two events with four electrons and one with four muons. It is curious that neither experiment found an event with two muons and two electrons, since the rate for this should equal the combined rate for events with four electrons or four muons. Very little background is expected in any of

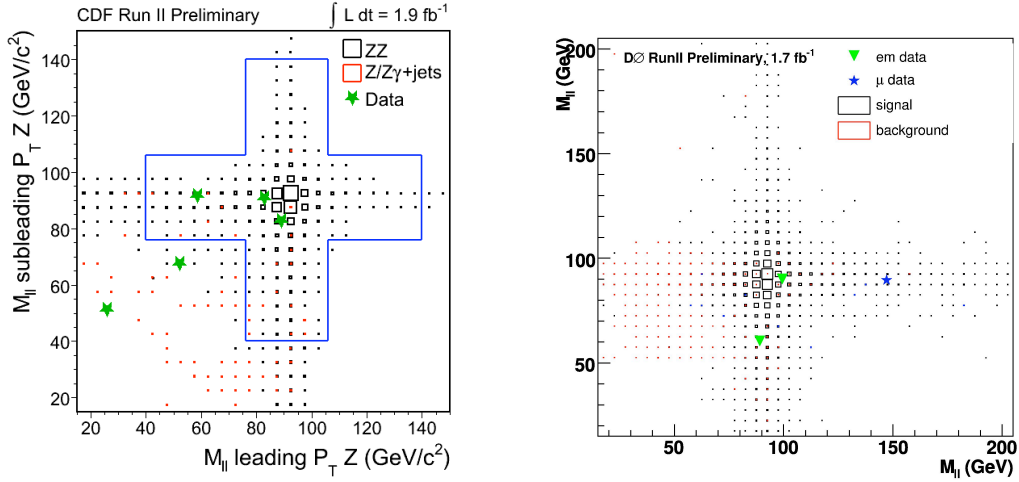


Figure 6: Masses of the two Z -boson candidates in ZZ candidate events as observed by CDF (left) and D0 (right).

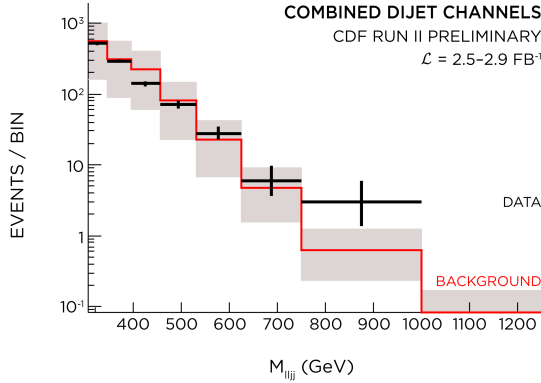


Figure 7: Four-body mass in ZZ resonance-production search. The points are the CDF data.

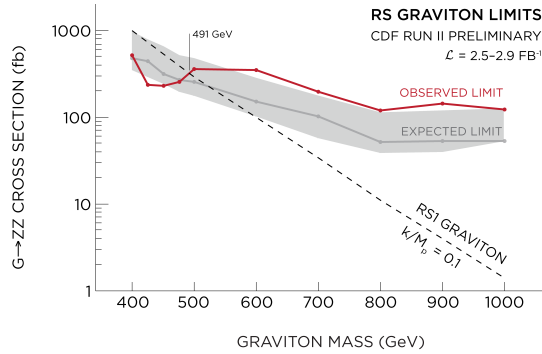


Figure 8: Cross section limit on R/S gravitons.

these channels. The measured cross sections are shown in Table 1 and the masses of the two lepton pairs are plotted against each other in Fig. 6.

As with WW and WZ production, it is possible for new physics to lead to ZZ resonance production. This has been searched for by CDF using expanded lepton acceptance and looking in the two-lepton plus two-jet channel as well as looking for four-lepton events. The two-lepton two-jet channel has substantial background, but a resonance should be apparent when the four-body mass is plotted (see Fig. 7). This search was used to set a lower limit on the mass of RS gravitons of 491 GeV/c^2 .

3 Summary

Diboson production at the Fermilab Tevatron has been studied by the CDF and D0 collaborations. All modes have been seen; their measured and expected cross sections are plotted in Fig. 9, and all are consistent with Standard Model expectations. The couplings are also consistent with Standard Model expectations, and limits have been placed on anomalous couplings that do not exist in the Standard Model. Searches for resonant production of dibosons have not found any excess, and limits have been placed on a number of new physics models that predict such production. In summary, all modes of diboson production have been observed at the Tevatron and all observables that have been studied are consistent with Standard Model

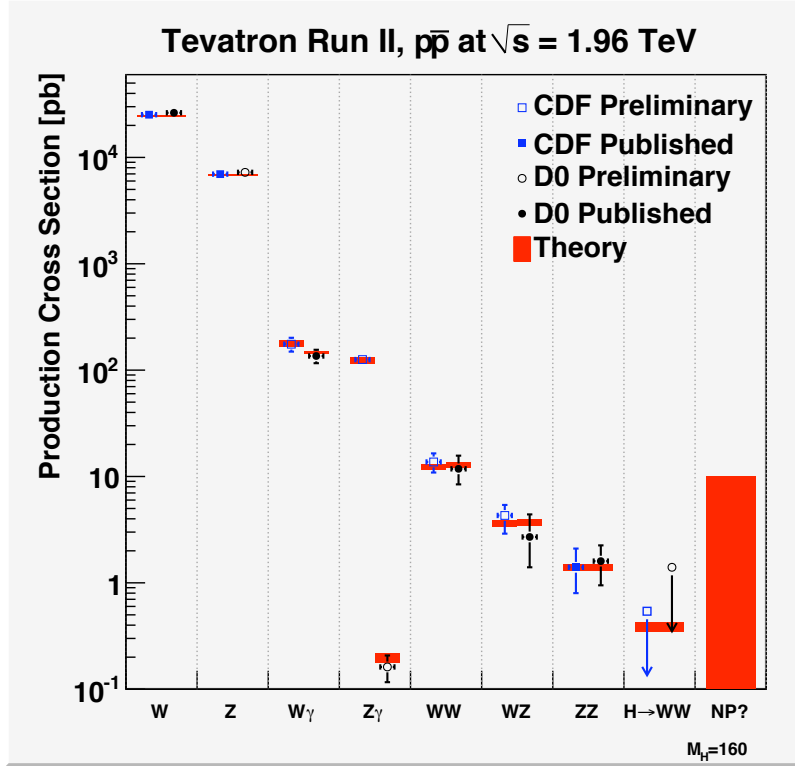


Figure 9: Measured (points) and expected (red bars) cross sections for diboson production, with single boson and Higgs production included for comparison.

expectations.

References

1. K.O. Mikaelian, M.A. Samuel, and D. Sahdev, Phys. Rev. Lett. **43**, 746 (1979).
2. V.M. Abazov *et al.* Phys. Rev. Lett. **100**, 241805 (2008).
3. K. Hagiwara, S. Ishihara, R. Szalapski, and D. Zeppenfeld, Phys. Rev. D **48**, 2182 (1993).
4. V.M. Abazov *et al.* Phys. Rev. D **76**, 111104(R) (2007).
5. V.M. Abazov *et al.* Phys. Rev. D **74**, 057101 (2006).
6. V.M. Abazov *et al.* Phys. Rev. Lett. **102**, 161801 (2009).
7. T. Aaltonen *et al.* Fermilab-Pub-09-054-E, submitted to Phys. Rev. D (2009).
8. V.M. Abazov *et al.* Fermilab-Pub-09-046-E, submitted to Phys. Rev. Lett. (2009).